Universiteit Leiden
The Netherlands

Fractional flow reserve in clinical practice: from wire-based invasive measurement to image-based computation

Tu, S.X.; Westra, J.; Adjedj, J.; Ding, D.X.; Liang, F.Y.; Xu, B.; ... ; Wijns, W.

Citation
Tu, S. X., Westra, J., Adjedj, J., Ding, D. X., Liang, F. Y., Xu, B., ... Wijns, W. (2020). Fractional flow reserve in clinical practice: from wire-based invasive measurement to image-based computation. *European Heart Journal*, *41*(34), 3271-3279. doi:10.1093/eurheartj/ehz918

Version:	Publisher's Version
License:	Creative Commons CC BY 4.0 license
Downloaded from:	https://hdl.handle.net/1887/3184467

Note: To cite this publication please use the final published version (if applicable).

ESC European Society of Cardiology

European Heart Journal (2020) **41**, 3271–3279
doi:10.1093/eurheartj/ehz918

CLINICAL REVIEW
Clinical update

Fractional flow reserve in clinical practice: from wire-based invasive measurement to image-based computation

Shengxian Tu [1]*†, Jelmer Westra [2†], Julien Adjedj [3,4†], Daixin Ding[1], Fuyou Liang[5,6], Bo Xu [7], Niels Ramsing Holm[2], Johan H.C. Reiber[8], and William Wijns [9]

[1]School of Biomedical Engineering, Shanghai Jiao Tong University, No. 1954 Hua Shan Road, Shanghai 200030, China; [2]Department of Cardiology, Aarhus University Hospital, Skejby, Palle Juul-Jensens Boulevard 99, 8200 Aarhus N, Denmark; [3]Cardiology Department, Arnault Tzanck Institute, 171 Rue du Commandant Gaston Cahuzac, 06700 Saint-Laurent-du-Var, France; [4]Cardiology Department, CHUV, Rue du Bugnon 46, 1011 Lausanne, Switzerland; [5]School of Naval Architecture, Ocean and Civil Engineering, Shanghai Jiao Tong University, 800 Dongchuan Road, Shanghai 200240, China; [6]Institute for Personalized Medicine, Sechenov University, 8-2 Trubetskaya st., Moscow 119991, Russia; [7]Catheterization Laboratories, Fu Wai Hospital, National Center for Cardiovascular Diseases, Chinese Academy of Medical Sciences, National Clinical Research Center for Cardiovascular Diseases, A 167, Beilishi Road, Xicheng District, Beijing 100037, China; [8]Division of Image Processing, Department of Radiology, Leiden University Medical Center, Albinusdreef 2, 2333 ZA Leiden, The Netherlands; and [9]The Lambe Institute for Translational Medicine and Curam, National University of Ireland Galway, University Road, Galway H91 TK3, Ireland

Received 13 July 2016; revised 27 July 2019; editorial decision 12 November 2019; accepted 4 December 2019; online publish-ahead-of-print 30 December 2019

Fractional flow reserve (FFR) and instantaneous wave-free ratio are the present standard diagnostic methods for invasive assessment of the functional significance of epicardial coronary stenosis. Despite the overall trend towards more physiology-guided revascularization, there remains a gap between guideline recommendations and the clinical adoption of functional evaluation of stenosis severity. A number of image-based approaches have been proposed to compute FFR without the use of pressure wire and induced hyperaemia. In order to better understand these emerging technologies, we sought to highlight the principles, diagnostic performance, clinical applications, practical aspects, and current challenges of computational physiology in the catheterization laboratory. Computational FFR has the potential to expand and facilitate the use of physiology for diagnosis, procedural guidance, and evaluation of therapies, with anticipated impact on resource utilization and patient outcomes.

Keywords Fractional flow reserve • Myocardial ischaemia • Coronary artery disease • IVUS • OCT and coronary angiogram

Introduction

Appropriate selection of patients and lesions in need of revascularization by stenting or bypass surgery is important. European practice guidelines advocate to perform pressure-based fractional flow reserve (FFR) or instantaneous wave-free ratio (iFR) measurements before revascularization, especially when prior testing for ischaemia is either inconclusive or unavailable.[1] Despite the overall trend favouring physiological guidance for revascularization, there remains a gap between guideline recommendations and the clinical adoption of functional stenosis evaluation.[2] To overcome the need for the use of disposable pressure wires during invasive functional testing, several computational methods for FFR estimation were developed. Presented solutions combine geometrical data from coronary angiography or intracoronary imaging and haemodynamic boundary conditions.[3–5] In this review, we present the scientific background for imaging-based computation of coronary physiological indices and aim to provide a theoretical understanding of advantages and limitations of these new methods. We further aim to present an overview of current evidence supporting their usefulness in clinical practice, both for diagnosis, procedural guidance, and evaluation of therapies.

Pressure-derived physiology

Fractional flow reserve quantifies the extent to which an epicardial obstruction limits maximal blood flow and predicts the potential benefit of medical therapy and revascularization. Fractional flow reserve is

* Corresponding author. Tel: +86 21 62932631, Fax: +86 21 62932156, Email: sxtu@sjtu.edu.cn

† The first three authors contributed equally to the study.

Published on behalf of the European Society of Cardiology. All rights reserved. © The Author(s) 2019. For permissions, please email: journals.permissions@oup.com.

Downloaded from https://academic.oup.com/eurheartj/article/41/34/3271/5690046 by Universiteit Leiden - LUMC user on 31 August 2023

measured as the ratio of the distal coronary pressure P*d* divided by the proximal coronary pressure, or aortic pressure, P*a* under maximal hyperaemic conditions during invasive coronary angiography (ICA).[6] Maximal hyperaemia abolishes the mechanisms responsible for the control of resting blood flow, in order to achieve a P*d*/P*a* ratio that equals the corresponding flow ratio governed by a linear relationship between perfusion pressure and hyperaemic flow.[7] Intracoronary nitrates (200 μg) are administered prior to advancing the pressure wire in the coronary artery to be interrogated, in order to prevent vasospasm. Hyperaemia can be induced by adenosine with continuous intravenous (IV) infusion (at 140 μg/kg/min) for 2 min, or intracoronary bolus (100 μg for the right coronary and 200 μg for the left coronary) or more recently with IV Regadenoson.[8] Despite a solid body of evidence and strong guideline recommendations, the global use of FFR remains inadequate.[9] Adoption of physiological assessment increased with the development and validation of iFR[10] that does not require the administration of hyperaemic agents. A large number of recently introduced new indexes based on resting pressure measured during various phases of the heart cycle are expected to provide similar diagnostic performance.[11]

Limitations of wire-based physiology

Pressure wire measurements require careful set-up and adherence to a standardized procedure. Confirming the waveform quality and absence of pressure drift is mandatory in order to obtain reliable FFR values.[12] In tortuous vessels, the pressure wire may induce an 'accordion' phenomenon, and therefore overestimate lesion severity. Fractional flow reserve is related to the total sum of vascular resistances. When only evaluating the pressure drop, assessment of haemodynamically significant epicardial disease can be influenced by microvascular dysfunction (*Figure 1*). Measurement of global coronary flow reserve incorporates the microcirculation but does not allow for discrimination between epicardial and microvascular disease (*Figure 1*). Measurement of microvascular resistance (e.g. index of microvascular resistance) can relate reduced coronary flow to microvascular dysfunction. Patients with microvascular dysfunction could benefit from microvasculature-targeted therapy. Combined moderate epicardial and microvascular disease constitutes a particular challenge, as myocardial blood flow will most likely be reduced (*Figure 1*). The optimal clinical management in this situation is still unclear as neither percutaneous coronary intervention (PCI) nor microvascular-focused therapy might fully relieve ischaemia. The theoretical concept of microvascular disease affecting epicardial disease is similar to assessment of tandem-lesions where the distal stenosis will act as a resistor to the proximal stenosis hiding part of the full ischaemic potential. Moderate epicardial disease can be associated with low FFR values in vessels supplying large perfusion territories, with an excessive response to hyperaemia driven by a low hyperaemic microvascular resistance (*Figure 1*).

Computation of pressure gradient and fractional flow reserve: scientific background

Computation of pressure gradient and FFR in diseased coronary arteries generally consists of three steps: (i) reconstructing geometric models based on coronary images and defining the range of computational domain (i.e. geometric boundary); (ii) selecting a haemodynamic modelling method; and (iii) prescribing haemodynamic boundary conditions (*Take home figure*). Supplementary material online, *Table S1* summarizes the key methodological aspects of each modality. For further details on the individual approaches, we refer to the Supplementary material online.

Geometric model reconstructed from three-dimensional coronary angiography

Three-dimensional quantitative coronary angiography (3D-QCA) can overcome some inherent limitations of standard two-dimensional angiography, such as vessel foreshortening and out-of-plane magnification error. Three-dimensional quantitative coronary angiography reconstructions are based on two or more angiographic projections (Supplementary material online, *Table S1*).[13–15] The lumen of the stenotic coronary artery segment is reconstructed in 3D by assuming that the cross-section is elliptical shape. Meanwhile, the reference lumen, i.e. the healthy lumen free of stenosis, is reconstructed in 3D by assuming that the cross-sectional shape is circular. If side branches are included in model reconstruction, the reference diameter can be adjusted to represent the 'step down' phenomenon at bifurcations.[16] Otherwise, a linear tapering of the reference diameter is assumed.

Geometric model reconstructed from intracoronary imaging data

Intravascular imaging techniques, such as optical coherence tomography (OCT) and intravascular ultrasound (IVUS), provide cross-sectional images of the coronary artery with high spatial resolution, allowing both lumen delineation and geometry reconstruction using commercially available solutions[5,17] or in-house software.[18–21] Ostia of side branches can be included in the reconstructed model to represent the reference step-down phenomenon at bifurcations.[5] *Figure 2* shows a case example of geometry derived from intracoronary imaging and 3D-QCA with the computational results co-registered with angiography and OCT.

Geometric model reconstructed from fused coronary angiographic and intracoronary imaging data

The fidelity of angiography-derived 3D reconstructions can be compromised by the elliptical shape assumption in stenotic coronary artery segments. This issue can be overcome through fusion of information derived from ICA with intracoronary imaging for true geometric reconstructions (*Take home figure*).[22] Clinical application of systems based on geometric fusion awaits higher degree of automation.

General modelling method for coronary blood flow

Coronary blood flow is pulsatile in nature. However, solving pulsatile blood flow is more cumbersome than steady flow. Transient computational fluid dynamics (CFD) analysis involves the solution of nonlinear partial differential equations with million degrees of freedom that generally requires a computational time of 12–24 h. For these reasons, pulsation of blood flow is often ignored. This is justified by the

Downloaded from https://academic.oup.com/eurheartj/article/41/34/3271/5690046 by Universiteit Leiden - LUMC user on 31 August 2023

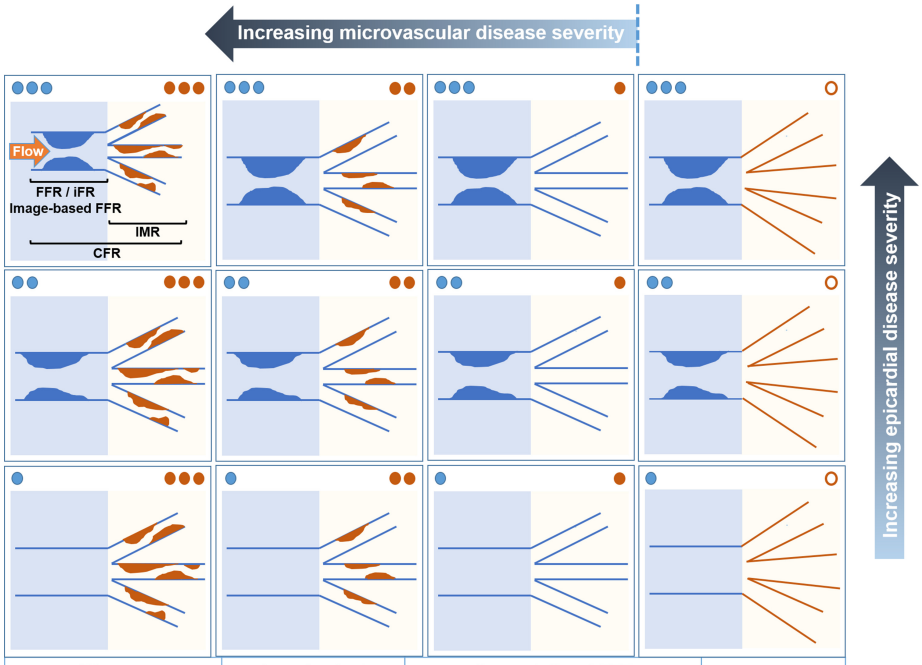

Disease		Invasive test			Computational FFR		Optimal clinical decision
Epicardial stenosis	Microcirculatory dysfunction	FFR	IMR	CFR	Patient-averaged flow	Patient-specific flow	
●●●	●●●	?	?	+	+	?	PCI and MOMT
●●●	●●	?	−	+	+	?	PCI
●●●	●	+	−	+	+	+	PCI
●●●	○	+	−	?	+	+	PCI
●●	●●●	−	+	+	−	−	MOMT
●●	●●	−	−	+	−	−	PCI or MOMT
●●	●	−	−	−	−	−	OMT
●●	○	?	−	−	−	−	OMT[a]
●	●●●	−	+	+	−	−	MOMT
●	●●	−	−	−	−	−	OMT
●	●	−	−	−	−	−	OMT
●	○	−	−	−	−	−	OMT

Figure 1 Simplified differential physiological status and optimal treatment of epicardial and microvascular disease as assessed in the catheterization laboratory. Combinations of different physiological severity of epicardial and microcirculatory disease. The epicardial disease severity is the same within each row and decreases from top to the bottom row. The microvascular dysfunction severity is the same within each column and decreases from left to right except for the rightmost column. The rightmost column represents microcirculation with excessive reaction to hyperaemia. −, non-significant; ?, uncertain; +, significant; CFR, coronary flow reserve; FFR, fractional flow reserve; iFR, instantaneous wave-free ratio; IMR, index of microvascular resistance; MOMT, microcirculation-target optimal medicine therapy; OMT, optimal medicine therapy; PCI, percutaneous coronary intervention. [a]Optimal treatment strategy under current investigation (ClinicalTrials.gov Identifier: NCT02328820).

fact that *in vivo* measurement of FFR is based on mean blood pressures averaged over several cardiac cycles.

Two main fluid dynamics models are used to compute FFR: (i) 3D Navier–Stokes equation-based CFD models and (ii) empirical fluid dynamic equations based on reduced-order models. Three-dimensional CFD models are more detailed and have higher spatial resolution[13,14,17] but reduced-order models are more suitable for clinical use owing to shorter computational time[5,15,20,21,23] (Supplementary material online, *Table S1*).

Inlet boundary conditions

Frequently applied boundary conditions at model inlet are pressure or flow, or a combination of them. Inlet pressure can be determined by patient-specific measurements or population-averaged data. Hyperaemic flow rates extracted directly from imaging modalities[5,14,17,22,23] or estimated from resting haemodynamic conditions and physiological assumptions are feasible alternatives.[15,18–20]

Outlet boundary conditions

Outlet boundary conditions are generally prescribed either through coupling the outlet(s) with a model of downstream micro-vessels[24] or by fixing a blood flow rate at the outlet(s).[5,14,18,20–23,25] The most frequently employed modelling method for coronary microcirculation is the lumped-parameter method in which generic one-size-fits-all parameters are used to characterize the overall impedance, resistance and compliance of the microcirculation.[15,19]

Downloaded from https://academic.oup.com/eurheartj/article/41/34/3271/5690046 by Universiteit Leiden - LUMC user on 31 August 2023

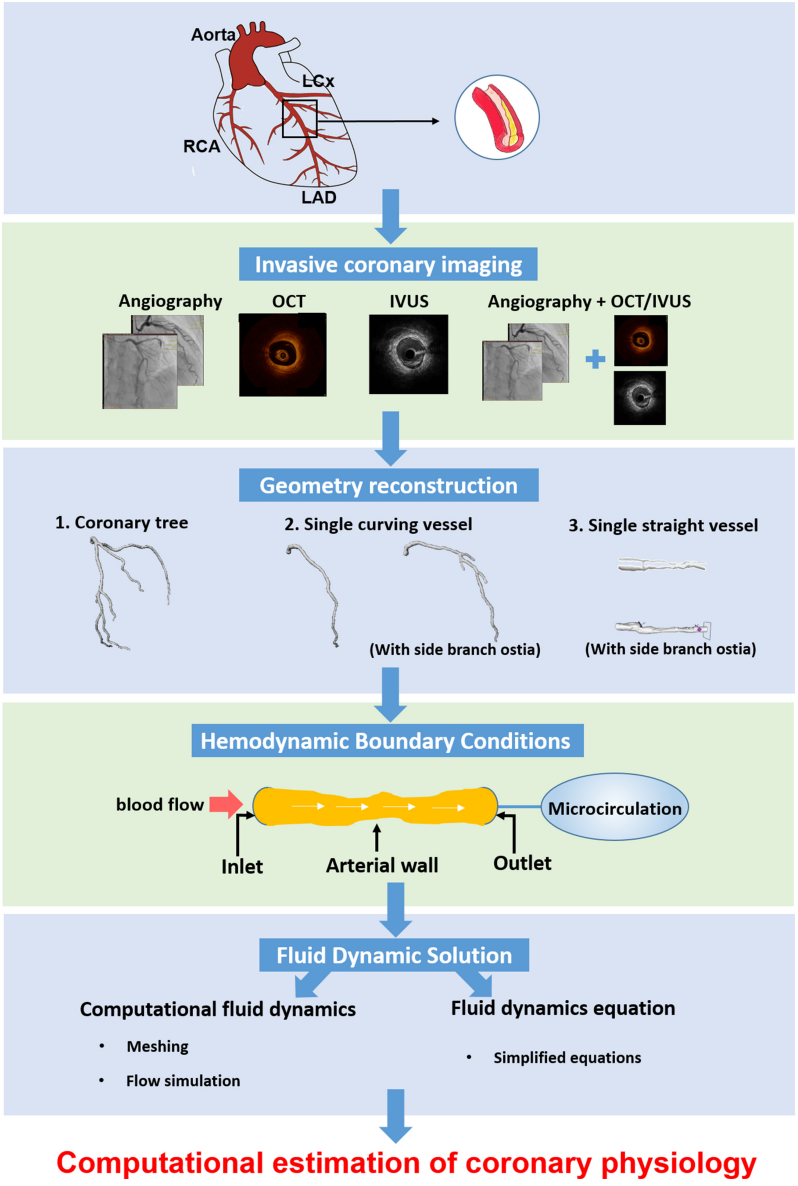

Take home figure Overview of methodological aspects in computational physiology. Computation of FFR requires three major steps: (i) geometry reconstruction; (ii) applying haemodynamic boundary conditions; and (iii) employing fluid dynamics solutions. CFD, computational fluid dynamics; FFR, fractional flow reserve; IVUS, intravascular ultrasound; LAD, left anterior descending artery; LCx, left circumflex; OCT, optical coherence tomography; RCA, right coronary artery.

Clinical validation

Currently, described modalities were predominantly evaluated in studies assessing the diagnostic performance by paired measurements with FFR as the reference standard (*Figure 3*, Supplementary material online, *Table S2*). Reduced accuracy and repeatability around the diagnostic cut-off for the FFR standard provides a theoretical ceiling for the maximum achievable diagnostic accuracy.[26] Importantly, the prognostic impact of 'false-negative' and 'false-positive' computational physiology estimates is not well defined and may partly be related to limitations of wire-based physiology as previously discussed (*Figure 1*). For feasibility and analysis time, it is important to distinguish between processing time consisting of pure 'computer-work' and total analysis time that includes manual interaction (Supplementary material online).

Diagnostic performance

Invasive coronary angiography-derived FFR has a good agreement and diagnostic performance, calculated on-line or off-line and shows diagnostic accuracy estimates between 86% and 97% with wire-based FFR as the reference standard (Supplementary material online,

Downloaded from https://academic.oup.com/eurheartj/article/41/34/3271/5690046 by Universiteit Leiden - LUMC user on 31 August 2023

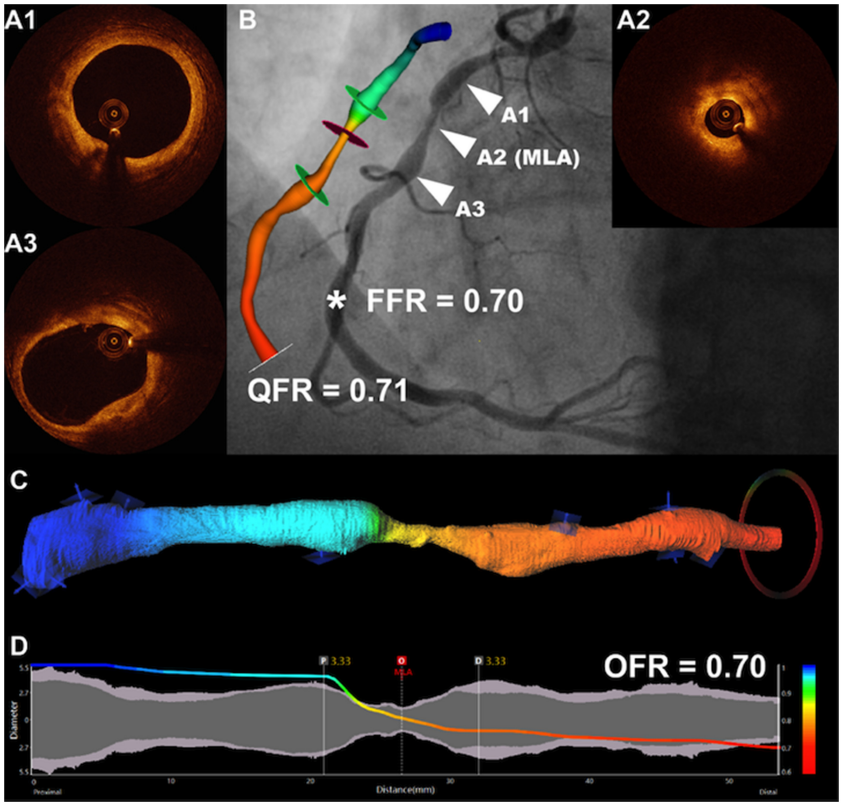

Figure 2 Case example of angiography-derived (quantitative flow ratio) and optical coherence tomography-derived (OFR) fractional flow reserve, with co-registration to coronary angiography and comparison with invasively measured wire-based fractional flow reserve. Computation of quantitative flow ratio and optical coherence tomography-based fractional flow reserve. Wire-based fractional flow reserve was measured at 0.70. (*A1–A3*) Positions on the optical coherence tomography-pullback, including minimal lumen area, which correspond to *A1–A3* in *B*. The computed quantitative flow ratio and optical coherence tomography-based fractional flow reserve values are colour-coded and superimposed on the three-dimensional quantitative coronary angiography reconstruction in *B* and the three-dimensional optical coherence tomography reconstruction in *C*. A virtual pressure pullback is provided to identify the precise location of pressure-drops along the vessel segment of interest in *D*.

Table S2). Recent meta-analysis found no difference in diagnostic performance for various ICA-derived FFR methods but head-to-head comparison of different methods is lacking.[27] The FAVOR II China and FAST-FFR study assessed the in-procedure diagnostic performance of quantitative flow ratio (QFR) and FFRangio. Both studies met their pre-specified performance goals.[3,28] The FAVOR II E-J proved that in-procedure QFR is superior to standard two-dimensional quantitative coronary angiography.[2] Recent data documented that FFRangio is reliable in multivessel disease.[29] Diagnostic performance results for physiology derived from intracoronary imaging are predominantly based on retrospective data with diagnostic accuracy estimates ranging from 88% to 94% and area under the receiver operating characteristic curve (AUC) of 0.93 (Supplementary material online, *Table S2*).

Diagnostic performance in specific patient and lesion subsets

The diagnostic concordance between QFR and FFR is reduced in patients with microcirculatory dysfunction defined as index of microvascular resistance >23 U.[30] This fits with findings illustrating an impaired concordance between QFR and FFR in vessels supplying territories with previous myocardial infarction.[31] It further appears that all modalities show increased scatter for lower FFR values; a phenomenon that is also known for other techniques when compared with FFR (e.g. CT-FFR).[32] In the acute physiological evaluation of non-culprit lesions in patients with ST-segment elevation myocardial infarction (STEMI) and multivessel disease, QFR showed good diagnostic agreement with FFR measured in a staged setting in proof-of-concept studies.[33,34]

Clinical outcome data

Limited data are available on the correlation between clinical outcome and ICA-derived FFR approaches, with all existing evidence from studies specifically characterizing the QFR solution. Functional SYNTAX score calculated by QFR in retrospective analysis of SYNTAX II study indicated superior prediction of a patient-oriented composite endpoint (PoCE) in patients with multivessel disease, when compared with the classical anatomical SYNTAX score [AUC 0.68 (0.50–0.87) vs. 0.56 (0.37–0.75), $P = 0.002$].[35] A recent study assessed the prognostic value of three-vessel QFR (3V-QFR) in

Downloaded from https://academic.oup.com/eurheartj/article/41/34/3271/5690046 by Universiteit Leiden - LUMC user on 31 August 2023

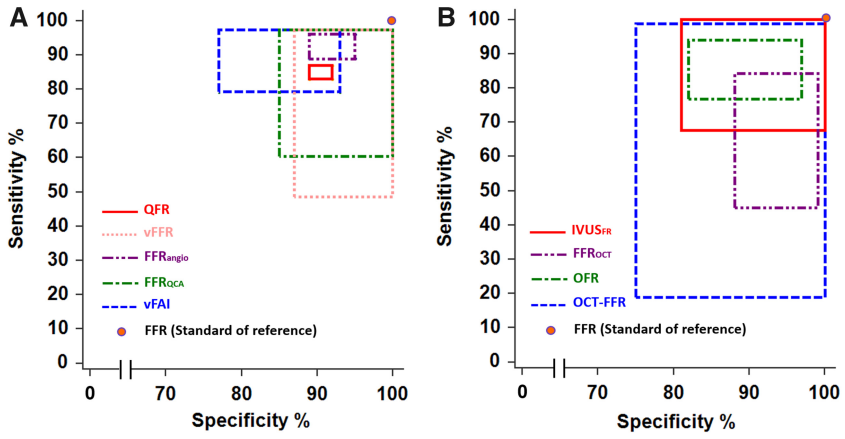

Figure 3 Sensitivity and specificity of (*A*) coronary angiography-derived and (*B*) intracoronary imaging-derived computational fractional flow reserve compared with invasively measured wire-based fractional flow reserve as the standard of reference. Pooled analysis was performed to derive sensitivity and specificity of each computed fractional flow reserve technique based on available validation studies (Supplementary material online, *Table S3*). Each rectangle in the panels represents the 95% confidence interval of sensitivity and specificity for each method. Number of studies and overall vessels for pooled analysis for each technique are as follows: QFR, 16 studies/3887 vessels; FFRangio, 3 studies/623 vessels; vFFR, 1 study/35 vessels; FFR_{QCA}, 1 study/77 vessels; vFAI, 1 study/139 vessels; OFR, 1 study/125 vessels; FFR_{OCT}, 1 study/92 vessels; OCT-FFR, 1 study/17 vessels; $IVUS_{FR}$, 1 study/34 vessels. FFR, fractional flow reserve; OFR, OCT-based FFR; QFR, quantitative flow ratio; vFAI, virtual functional assessment index; vFFR, virtual fractional flow reserve.

patients with stable coronary artery disease and found that major adverse cardiac events (MACE) were predicted in a continuous manner independently from revascularization decisions.[36] In practical terms, 3V-QFR is actually easier to obtain than wire-based FFR that requires separate instrumentation of each major vessel. In a proof-of-concept study, the use of functional SYNTAX score based on QFR was able to predict PoCE in STEMI patients with multivessel disease and at least one non-culprit lesion was left untreated.[34]

Clinical application of computed coronary physiology

Optimized referral of patients from diagnostic catheterization laboratories

In many areas, hospitals have diagnostic catheterization laboratories not able or allowed to perform pressure wire-based functional testing. Here, ICA-based approaches may be of importance in ensuring sole referral of patients with haemodynamic significant coronary artery disease. This could lead to a reduction in secondary ICA procedures not followed by revascularization. A retrospective report on referral after ICA with and without QFR showed a 50% reduction in patient referrals for a second ICA, while 22% of the referred patients could undergo direct PCI based on the QFR-treat cut-point (≤0.77) as identified in the FAVOR II E-J study.[2,37]

Evaluation of non-culprit lesions in patients with acute myocardial infarction

The timing and method for assessing haemodynamic significance of non-culprit lesions in STEMI patients with multivessel disease remains a subject under investigation (ClinicalTrials.gov NCT03298659 and NCT02862119). Fractional flow reserve-guided complete revascularization showed beneficial cardiovascular outcomes when compared with treatment of the culprit-lesion only.[38] In theory, the accuracy of FFR in the setting of MI is still debated as full hyperaemia may not be achieved due to a disturbed microvascular function (*Figure 1*). Notably, ICA-derived computational physiology for non-culprit lesions is similar in the acute vs. staged settings.[33,34] This raises the question whether computational solutions based on- (or allowing for) fixed-flow assumptions represent a better epicardial-specific index in this setting (*Figure 1*). The use of imaging-derived physiology may reduce the number of down-stream procedures for this patient group and will be the subject of future studies.

Percutaneous coronary intervention optimization

Most studies have shown that post-PCI FFR <0.90 or small increase between pre- and post-PCI FFR is associated with worse clinical outcome.[39–41] It is therefore reasonable to expect imaging-derived physiology to play an increasingly important role in post-PCI evaluation, also given the good agreement with pre-stenting FFR. Suboptimal post-PCI FFR can be caused by multiple factors such as unmasking of a 2nd lesion, diffuse disease and procedure-related factors (e.g. flow disturbance inside the stent itself). Optical coherence tomography provides more precise information on stent positioning, stent expansion, intimal injuries, and healing patterns when compared with ICA. Hence, post-PCI computation of FFR using intracoronary imaging approaches can incorporate stent malapposition and underexpansion.[5] It is therefore plausible that combined intracoronary imaging and imaging-derived physiology will play an important future

Downloaded from https://academic.oup.com/eurheartj/article/41/34/3271/5690046 by Universiteit Leiden - LUMC user on 31 August 2023

role in optimizing PCI and establishing objective criteria for procedural 'success' and value-based health care implementation.

Important practical aspects and current challenges

Image acquisition

Angiographic image quality is of utmost importance for ICA-based approaches and attention should be paid to ensure optimal contrast filling, reduced panning, minimal foreshortening, and vessel overlap. Rotational angiography provides a potential solution but is not widely available. Standardized acquisition guidelines may improve the feasibility exemplified by the higher exclusion rate in retrospective studies compared with reports from prospective studies.[28,35] For intracoronary imaging-based solutions, scanning of all stenoses located in the interrogated vessel may be required. During ideal intracoronary imaging procedures, the OCT/IVUS imaging catheter should be advanced distally to the interrogated stenosis landing at normal coronary segment and the pullback should cover all diseased segments up to the most proximal normal segment. Failure to include all the stenoses will lead to underestimation of lesion severity. The widest available OCT system in Europe (ILUMIEN, Abbott, USA) covers a maximum pullback length of 75 mm, which may constitute a limitation in assessing longer lesions. Of note, analysis of OCT-based FFR (OFR) allows for combination of two OCT pullbacks to assess vessel-based OFR. Images acquired by slow vs. high pullback speed may render different lesion coverage and create a potential source of variance due to cardiac motion.

Ideal vs. practical estimation of boundary conditions: does one size fit all?

One of the greatest challenges for computational physiology is developing accurate boundary conditions reflecting the coronary blood flow dynamics where large inter-patient variation may occur. A recent study illustrated that variability in coronary microvasculature resistance influences virtual FFR to a larger degree than variability in coronary anatomy.[24] However, ideal modelling of the microvascular bed requires patient-specific data and increased computational complexity that altogether hamper feasibility. Since FFR is affected by microvascular resistance, virtual solutions using more or less generalized boundary conditions reflecting microvascular resistance and fixed flow will therefore be prone to larger discrepancy with FFR in cases with impaired microcirculatory dysfunction, such as vessels supplying territories with previous MI (*Figure 1*). The question is whether the discrepancy is in favour of FFR or computational approaches. Coronary flow reserve/FFR discordance may be present in case of microvascular dysfunction where FFR-guided revascularization may not always lead to the correct treatment (*Figure 1*). On the contrary, FFR might be falsely positive (abnormal) for donor vessels with mild epicardial disease in chronic total occlusion (CTO) patients. Instead of stenting the donor vessel, the proper clinical decision might be to open the CTO, after which procedure the 'abnormal' FFR in the donor vessel may normalize.

Future perspectives

Randomized trials are required to demonstrate the clinical value of imaging-based computed physiology for guidance of PCI and other potential indications. Cost-effectiveness analyses are pending. Two ongoing randomized trials are assessing the clinical value of QFR as diagnostic tool in patients with stable coronary artery disease. FAVOR III Europe-Japan (ClinicalTrials.gov NCT03729739) assesses if a QFR-guided diagnostic strategy yields non-inferior 12-month clinical outcomes compared with a standard FFR-guidance. FAVOR III China (ClinicalTrial.gov NCT03656848) assesses if a QFR-guided PCI strategy results in superior clinical outcome (MACE) compared with standard angiography-guided PCI (FFR is not routinely used in China). Computational FFR is expected to widen the usability and adoption of physiological guidance, further enabling improved patient outcomes and more appropriate resource utilization.

Supplementary material

Supplementary material is available at *European Heart Journal* online.

Acknowledgements

S.T. acknowledges the support the Natural Science Foundation of China (81871460) and by the Program of Shanghai Technology Research Leader. J.W. acknowledges the support from Aarhus University (PhD scholarship). W.W. is the recipient of a Research Professorship Award, by Science Foundation Ireland.

Conflict of interest: S.T. received a research grant from Medis medical imaging and Pulse medical imaging technology. J.R is Prof. of medical imaging at the Leiden University Medical Center and CSO of Medis medical imaging technology. W.W. received non-financial supports from Medis medical imaging and HeartFlow, and grants from Abbott, Volcano, and Boston Scientific. N.H. received institutional research grants from Boston Scientific, St Jude Medical, and Medis medical imaging. J.W. received travel support and consultant fees from Medis medical imaging. All other authors declared no conflict of interest.

References

1. Neumann F-J, Sousa-Uva M, Ahlsson A, Alfonso F, Banning AP, Benedetto U, Byrne RA, Collet J-P, Falk V, Head SJ, Jüni P, Kastrati A, Koller A, Kristensen SD, Niebauer J, Richter DJ, Seferović PM, Sibbing D, Stefanini GG, Windecker S, Yadav R, Zembala MO; ESC Scientific Document Group. 2018 ESC/EACTS guidelines on myocardial revascularization. *Eur Heart J* 2019;**40**:87–165.
2. Westra J, Andersen BK, Campo G, Matsuo H, Koltowski L, Eftekhari A, Liu T, Di Serafino L, Di Girolamo D, Escaned J, Nef H, Naber C, Barbierato M, Tu S, Neghabat O, Madsen M, Tebaldi M, Tanigaki T, Kochman J, Somi S, Esposito G, Mercone G, Mejia-Renteria H, Ronco F, Bøtker HE, Wijns W, Christiansen EH, Holm NR. Diagnostic performance of in-procedure angiography-derived quantitative flow reserve compared to pressure-derived fractional flow reserve: the FAVOR II Europe-Japan study. *J Am Heart Assoc* 2018;**7**:e009603.
3. Fearon WF, Achenbach S, Engstrom T, Assali A, Shlofmitz R, Jeremias A, Fournier S, Kirtane AJ, Kornowski R, Greenberg G, Jubeh R, Kolansky DM, McAndrew T, Dressler O, Maehara A, Matsumura M, Leon MB, De Bruyne B. Accuracy of fractional flow reserve derived from coronary angiography. *Circulation* 2019;**139**:477–484.
4. Westra J, Tu S, Campo G, Qiao S, Matsuo H, Qu X, Koltowski L, Chang Y, Liu T, Yang J, Andersen BK, Eftekhari A, Christiansen EH, Escaned J, Wijns W, Xu B, Holm NR. Diagnostic performance of quantitative flow ratio in prospectively enrolled patients: an individual patient-data meta-analysis. *Catheter Cardiovasc Interv* 2019;**94**:693–701.

Downloaded from https://academic.oup.com/eurheartj/article/41/34/3271/5690046 by Universiteit Leiden - LUMC user on 31 August 2023

5. Yu W, Huang J, Jia D, Chen S, Raffel OC, Ding D, Tian F, Kan J, Zhang S, Yan F, Chen Y, Bezerra HG, Wijns W, Tu S. Diagnostic accuracy of intracoronary optical coherence tomography-derived fractional flow reserve for assessment of coronary stenosis severity. *EuroIntervention* 2019;**15**:189–197.
6. Pijls NH, van Son JA, Kirkeeide RL, De Bruyne B, Gould KL. Experimental basis of determining maximum coronary, myocardial, and collateral blood flow by pressure measurements for assessing functional stenosis severity before and after percutaneous transluminal coronary angioplasty. *Circulation* 1993;**87**:1354–1367.
7. De Bruyne B, Baudhuin T, Melin JA, Pijls NH, Sys SU, Bol A, Paulus WJ, Heyndrickx GR, Wijns W. Coronary flow reserve calculated from pressure measurements in humans. Validation with positron emission tomography. *Circulation* 1994;**89**:1013–1022.
8. Pradeep A, Vincent MF, Parul BP, Morris DL. Comparison of intravenous adenosine and intravenous regadenoson for the measurement of pressure-derived coronary fractional flow reserve. *EuroIntervention* 2013;**8**:1166–1171.
9. Tebaldi M, Biscaglia S, Fineschi M, Musumeci G, Marchese A, Leone AM, Rossi ML, Stefanini G, Maione A, Menozzi A, Tarantino F, Lodolini V, Gallo F, Barbato E, Tarantini G, Campo G. Evolving routine standards in invasive hemodynamic assessment of coronary stenosis: the Nationwide Italian SICI-GISE Cross-Sectional ERIS Study. *J Am Coll Cardiol Intv* 2018;**11**:1482–1491.
10. Davies JE, Sen S, Dehbi H-M, Al-Lamee R, Petraco R, Nijjer SS, Bhindi R, Lehman SJ, Walters D, Sapontis J, Janssens L, Vrints CJ, Khashaba A, Laine M, Van Belle E, Krackhardt F, Bojara W, Going O, Härle T, Indolfi C, Niccoli G, Ribichini F, Tanaka N, Yokoi H, Takashima H, Kikuta Y, Erglis A, Vinhas H, Canas Silva P, Baptista SB, Alghamdi A, Hellig F, Koo B-K, Nam C-W, Shin E-S, Doh J-H, Brugaletta S, Alegria-Barrero E, Meuwissen M, Piek JJ, van Royen N, Sezer M, Di Mario C, Gerber RT, Malik IS, Sharp ASP, Talwar S, Tang K, Samady H, Altman J, Seto AH, Singh J, Jeremias A, Matsuo H, Kharbanda RK, Patel MR, Serruys P, Escaned J. Use of the instantaneous wave-free ratio or fractional flow reserve in PCI. *N Engl J Med* 2017;**376**:1824–1834.
11. Van't Veer M, Pijls NHJ, Hennigan B, Watkins S, Ali ZA, De Bruyne B, Zimmermann FM, van Nunen LX, Barbato E, Berry C, Oldroyd KG. Comparison of different diastolic resting indexes to iFR: are they all equal? *J Am Coll Cardiol* 2017;**70**:3088–3096.
12. Toth GG, Johnson NP, Jeremias A, Pellicano M, Vranckx P, Fearon WF, Barbato E, Kern MJ, Pijls NH, De Bruyne B. Standardization of fractional flow reserve measurements. *J Am Coll Cardiol* 2016;**68**:742–753.
13. Morris PD, Ryan D, Morton AC, Lycett R, Lawford PV, Hose DR, Gunn JP. Virtual fractional flow reserve from coronary angiography: modeling the significance of coronary lesions: results from the VIRTU-1 (VIRTUal Fractional Flow Reserve From Coronary Angiography) study. *J Am Coll Cardiol Intv* 2013;**6**:149–157.
14. Tu S, Barbato E, Köszegi Z, Yang J, Sun Z, Holm NR, Tar B, Li Y, Rusinaru D, Wijns W, Reiber JHC. Fractional flow reserve calculation from 3-dimensional quantitative coronary angiography and TIMI frame count: a fast computer model to quantify the functional significance of moderately obstructed coronary arteries. *JACC Cardiovasc Interv* 2014;**7**:768–777.
15. Pellicano M, Lavi I, De Bruyne B, Vaknin-Assa H, Assali A, Valtzer O, Lotringer Y, Weisz G, Almagor Y, Xaplanteris P, Kirtane AJ, Codner P, Leon MB, Kornowski R. Validation study of image-based fractional flow reserve during coronary angiography. *Circ Cardiovasc Interv* 2017;**10**:e005259.
16. Tu S, Echavarria-Pinto M, von Birgelen C, Holm NR, Pyxaras SA, Kumsars I, Lam MK, Valkenburg I, Toth GG, Li Y, Escaned J, Wijns W, Reiber JHC. Fractional flow reserve and coronary bifurcation anatomy: a novel quantitative model to assess and report the stenosis severity of bifurcation lesions. *JACC Cardiovasc Interv* 2015;**8**:564–574.
17. Ha J, Kim JS, Lim J, Kim G, Lee S, Lee JS, Shin DH, Kim BK, Ko YG, Choi D, Jang Y, Hong MK. Assessing computational fractional flow reserve from optical coherence tomography in patients with intermediate coronary stenosis in the left anterior descending artery. *Circ Cardiovasc Interv* 2016;**9**:e003613.
18. Bezerra CG, Hideo-Kajita A, Bulant CA, Maso-Talou GD, Mariani J Jr Pinton FA, Falcão BAA, Esteves-Filho A, Franken M, Feijóo RA, Kalil-Filho R, Garcia-Garcia HM, Blanco PJ, Lemos PA. Coronary fractional flow reserve derived from intravascular ultrasound imaging: validation of a new computational method of fusion between anatomy and physiology. *Catheter Cardiovasc Interv* 2019;**93**:266–274.
19. Lee KE, Lee SH, Shin E-S, Shim EB. A vessel length-based method to compute coronary fractional flow reserve from optical coherence tomography images. *BioMed Eng Online* 2017;**16**:83.
20. Seike F, Uetani T, Nishimura K, Kawakami H, Higashi H, Aono J, Nagai T, Inoue K, Suzuki J, Kawakami H, Okura T, Yasuda K, Higaki J, Ikeda S. Intracoronary optical coherence tomography-derived virtual fractional flow reserve for the assessment of coronary artery disease. *Am J Cardiol* 2017;**120**:1772–1779.
21. Seike F, Uetani T, Nishimura K, Kawakami H, Higashi H, Fujii A, Aono J, Nagai T, Inoue K, Suzuki J, Inaba S, Okura T, Yasuda K, Higaki J, Ikeda S. Intravascular ultrasound-derived virtual fractional flow reserve for the assessment of myocardial ischemia. *Circ J* 2018;**82**:815–823.
22. Li Y, Gutiérrez-Chico JL, Holm NR, Yang W, Hebsgaard L, Christiansen EH, Mæng M, Lassen JF, Yan F, Reiber JHC, Tu S. Impact of side branch modeling on computation of endothelial shear stress in coronary artery disease: coronary tree reconstruction by fusion of 3D angiography and OCT. *J Am Coll Cardiol* 2015;**66**:125–135.
23. Tu S, Westra J, Yang J, von Birgelen C, Ferrara A, Pellicano M, Nef H, Tebaldi M, Murasato Y, Lansky A, Barbato E, van der Heijden LC, Reiber JHC, Holm NR, Wijns W. Diagnostic accuracy of fast computational approaches to derive fractional flow reserve from diagnostic coronary angiography: the international multicenter FAVOR Pilot Study. *JACC Cardiovasc Interv* 2016;**9**:2024–2035.
24. Morris PD, Silva Soto DA, Feher JFA, Rafiroiu D, Lungu A, Varma S, Lawford PV, Hose DR, Gunn JP. Fast virtual fractional flow reserve based upon steady-state computational fluid dynamics analysis: results from the VIRTU-FAST Study. *JACC Basic Transl Sci* 2017;**2**:434–446.
25. Masdjedi K, van Zandvoort LJC, Balbi MM, Gijsen FJH, Ligthart JMR, Rutten MCM, Lemmert ME, Wilschut J, Diletti R, De Jaegere P, Zijlstra F, Van Mieghem NM, Daemen J. Validation of 3-dimensional quantitative coronary angiography based software to calculate fractional flow reserve: fast assessment of stenosis severity (FAST)-study. *EuroIntervention* 2019;doi:10.4244/EIJ-D-19-00466 (Epub ahead of print).
26. Petraco R, Sen S, Nijjer S, Echavarria-Pinto M, Escaned J, Francis DP, Davies JE. Fractional flow reserve-guided revascularization: practical implications of a diagnostic gray zone and measurement variability on clinical decisions. *JACC Cardiovasc Interv* 2013;**6**:222–225.
27. Collet C, Onuma Y, Sonck J, Asano T, Vandeloo B, Kornowski R, Tu S, Westra J, Holm NR, Xu B, de Winter RJ, Tijssen JG, Miyazaki Y, Katagiri Y, Tenekecioglu E, Modolo R, Chichareon P, Cosyns B, Schoors D, Roosens B, Lochy S, Argacha JF, van Rosendael A, Bax J, Reiber JHC, Escaned J, De Bruyne B, Wijns W, Serruys PW. Diagnostic performance of angiography-derived fractional flow reserve: a systematic review and Bayesian meta-analysis. *Eur Heart J* 2018;**39**:3314–3321.
28. Xu B, Tu S, Qiao S, Qu X, Chen Y, Yang J, Guo L, Sun Z, Li Z, Tian F, Fang W, Chen J, Li W, Guan C, Holm NR, Wijns W, Hu S. Diagnostic accuracy of angiography-based quantitative flow ratio measurements for online assessment of coronary stenosis. *J Am Coll Cardiol* 2017;**70**:3077–3087.
29. Omori H, Witberg G, Kawase Y, Tanigaki T, Okamoto S, Hirata T, Sobue Y, Ota H, Kamiya H, Okubo M, Valzer O, Kornowski R, Matsuo H. Angiogram based fractional flow reserve in patients with dual/triple vessel coronary artery disease. *Int J Cardiol* 2019;**283**:17–22.
30. Mejía-Rentería H, Lee JM, Lauri F, van der Hoeven NW, de Waard GA, Macaya F, Pérez-Vizcayno MJ, Gonzalo N, Jiménez-Quevedo P, Nombela-Franco L, Salinas P, Núñez-Gil I, del Trigo M, Goto S, Lee HJ, Liontou C, Fernández-Ortiz A, Macaya C, van Royen N, Koo B-K, Escaned J. Influence of microcirculatory dysfunction on angiography-based functional assessment of coronary stenoses. *JACC Cardiovasc Interv* 2018;**11**:741–753.
31. Emori H, Kubo T, Kameyama T, Ino Y, Matsuo Y, Kitabata H, Terada K, Katayama Y, Aoki H, Taruya A, Shimamura K, Ota S, Tanaka A, Hozumi T, Akasaka T. Diagnostic accuracy of quantitative flow ratio for assessing myocardial ischemia in prior myocardial infarction. *Circ J* 2018;**82**:807–814.
32. Cook CM, Petraco R, Shun-Shin MJ, Ahmad Y, Nijjer S, Al-Lamee R, Kikuta Y, Shiono Y, Mayet J, Francis DP, Sen S, Davies JE. Diagnostic accuracy of computed tomography-derived fractional flow reserve: a systematic review. *JAMA Cardiol* 2017;**2**:803–810.
33. Sejr-Hansen M, Westra J, Thim T, Christiansen EH, Eftekhari A, Kristensen SD, Jakobsen L, Gotberg M, Frobert O, van der Hoeven NW, Holm NR, Maeng M. Quantitative flow ratio for immediate assessment of nonculprit lesions in patients with ST-segment elevation myocardial infarction—an iSTEMI substudy. *Catheter Cardiovasc Interv* 2019;**94**:686–692.
34. Spitaleri G, Tebaldi M, Biscaglia S, Westra J, Brugaletta S, Erriquez A, Passarini G, Brieda A, Leone AM, Picchi A, Ielasi A, Girolamo DD, Trani C, Ferrari R, Reiber JHC, Valgimigli M, Sabate M, Campo G. Quantitative flow ratio identifies nonculprit coronary lesions requiring revascularization in patients with ST-segment-elevation myocardial infarction and multivessel disease. *Circ Cardiovasc Interv* 2018;**11**:e006023.
35. Asano T, Katagiri Y, Chang CC, Kogame N, Chichareon P, Takahashi K, Modolo R, Tenekecioglu E, Collet C, Jonker H, Appleby C, Zaman A, van Mieghem N, Uren N, Zueco J, Piek JJ, Reiber JHC, Farooq V, Escaned J, Banning AP, Serruys PW, Onuma Y. Angiography-derived fractional flow reserve in the SYNTAX II trial: feasibility, diagnostic performance of quantitative flow ratio, and clinical prognostic value of functional SYNTAX score derived from quantitative flow ratio in patients with 3-vessel disease. *JACC Cardiovasc Interv* 2019;**12**:259–270.
36. Hamaya R, Hoshino M, Kanno Y, Yamaguchi M, Ohya H, Sumino Y, Kanaji Y, Usui E, Murai T, Lee T, Yonetsu T, Hirao K, Kakuta T. Prognostic implication of three-vessel contrast-flow quantitative flow ratio in patients with stable coronary artery disease. *EuroIntervention* 2019;**15**:180–188.
37. Smit J, Koning G, van Rosendael A, Mahdiui ME, Mertens B, Jukema J, Delgado V, Reiber J, Bax JJ, Scholte A. Referral of patients for fractional flow reserve using

Downloaded from https://academic.oup.com/eurheartj/article/41/34/3271/5690046 by Universiteit Leiden - LUMC user on 31 August 2023

coronary contrast-flow quantitative flow ratio. *J Am Coll Cardiol* 2019;**123**:1722–1728.
38. Smits PC, Abdel-Wahab M, Neumann F-J, Boxma-de Klerk BM, Lunde K, Schotborgh CE, Piroth Z, Horak D, Wlodarczak A, Ong PJ, Hambrecht R, Angerås O, Richardt G, Omerovic E. Fractional flow reserve-guided multivessel angioplasty in myocardial infarction. *N Engl J Med* 2017;**376**:1234–1244.
39. Pijls NH, Klauss V, Siebert U, Powers E, Takazawa K, Fearon WF, Escaned J, Tsurumi Y, Akasaka T, Samady H, De Bruyne B. Coronary pressure measurement after stenting predicts adverse events at follow-up: a multicenter registry. *Circulation* 2002;**105**:2950–2954.
40. Fournier S, Ciccarelli G, Toth GG, Milkas A, Xaplanteris P, Tonino PAL, Fearon WF, Pijls NHJ, Barbato E, De Bruyne B. Association of improvement in fractional flow reserve with outcomes, including symptomatic relief, after percutaneous coronary intervention. *JAMA Cardiol* 2019;**4**:370–374.
41. Agarwal SK, Kasula S, Hacioglu Y, Ahmed Z, Uretsky BF, Hakeem A. Utilizing post-intervention fractional flow reserve to optimize acute results and the relationship to long-term outcomes. *JACC Cardiovasc Interv* 2016;**9**:1022–1031.

Downloaded from https://academic.oup.com/eurheartj/article/41/34/3271/5690046 by Universiteit Leiden - LUMC user on 31 August 2023

CARDIOVASCULAR FLASHLIGHT

doi:10.1093/eurheartj/ehaa518
Online publish-ahead-of-print 8 July 2020

Immersive virtual reality surgical planning of minimally invasive coronary artery bypass for Kawasaki disease

Amir H. Sadeghi *, Yannick J. H. J. Taverne, Ad J. J. C. Bogers , and Edris A. F. Mahtab

Department of Cardiothoracic Surgery, Thoraxcenter, Erasmus Medical Center Rotterdam, Room Rg-635, PO Box 2040, 3015 GD Rotterdam, The Netherlands

*Corresponding author. Tel: +31 10 7035411, Email: h.sadeghi@erasmusmc.nl

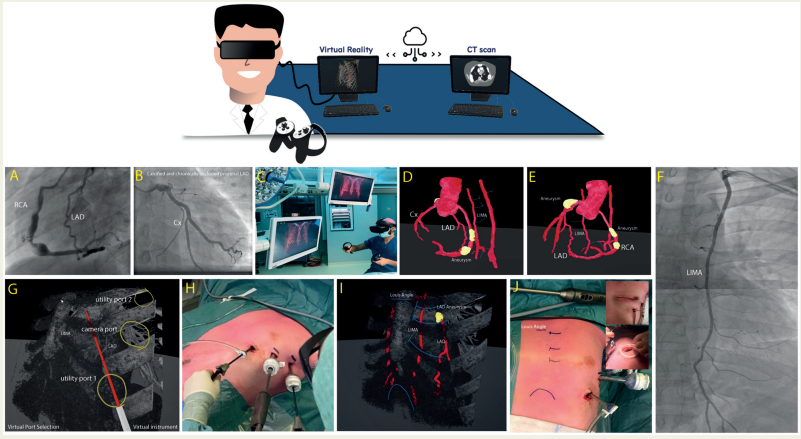

We present the rendering of a computed tomography (CT) scan in an immersive virtual reality (VR) environment for reviewing anatomy and preoperative planning of minimally invasive direct coronary artery bypass (MIDCAB). An 18-year-old man with a history of Kawasaki disease and associated left anterior descending (LAD) and right coronary artery (RCA) aneurysms, was referred to our multidisciplinary heart meeting to evaluate the necessity of coronary revascularization. The patient had no complaints, the electrocardiogram was normal and echocardiogram showed no resting regional wall motion abnormalities. Stress cardiac magnetic resonance imaging established subendocardial hypoperfusion defects in the LAD region without signs of myocardial fibrosis. A coronary angiography revealed a proximally calcified aneurysm and an occlusion of the LAD with collateral retrograde filling from the RCA and no abnormalities in the left circumflex (Cx) artery (*Panels A* and *B*, Supplementary material online, *Videos S1* and *S2*). Aneurysm formation of the left internal mammary artery (LIMA) was ruled out with angiography (*Panel F*). The patient was accepted for MIDCAB, LIMA to LAD coronary revascularization. To prepare for surgery, reconstructions of a CT scan were made by rendering 3D-VR images on our MedicalVR workstation (MedicalVR, Amsterdam, The Netherlands) (*Panel C*). An interactive reconstruction of the CT scan was made that enabled immersive-360° review of coronary anatomy in a head-mounted VR device (*Panels D* and *E*, Supplementary material online, *Video S3*). In addition, immersive VR was used to plan for the insertion location of thoracoscopic ports (for LIMA harvesting) and for determining the ideal location for anterior mini-thoracotomy (*Panels G–J*, Supplementary material online, *Videos S4–S6*) and direct off-pump MIDCAB using soft-tissue retractor. Cx, left circumflex artery; LAD, left anterior descending; LIMA, left internal mammary artery; RCA, right coronary artery.

Supplementary material is available at *European Heart Journal* online.

© The Author(s) 2020. Published by Oxford University Press on behalf of the European Society of Cardiology.
This is an Open Access article distributed under the terms of the Creative Commons Attribution Non-Commercial License (http://creativecommons.org/licenses/by-nc/4.0/), which permits non-commercial re-use, distribution, and reproduction in any medium, provided the original work is properly cited. For commercial re-use, please contact journals.permissions@oup.com